Effect of Spatial Dispersion on Surface Waves Propagating Along Graphene Sheets

Juan Sebastian Gomez-Diaz, *Member, IEEE*, Juan R. Mosig, *Fellow, IEEE*, and Julien Perruisseau-Carrier, *Senior Member, IEEE*

***Abstract*—We investigate the propagation of surface waves along a spatially dispersive graphene sheet, including substrate effects. The proposed analysis derives the admittances of an equivalent circuit of graphene able to handle spatial dispersion, using a nonlocal model of graphene conductivity. Similar to frequency-selective surfaces, the analytical admittances depend on the propagation constant of the waves traveling along the sheet. Dispersion relations for the supported TE and TM modes are then obtained by applying a transverse resonance equation. Application of the method demonstrates that spatial dispersion can dramatically affect the propagation of surface plasmons, notably modifying their mode confinement and increasing losses, even at frequencies where intraband transitions are the dominant contribution to graphene conductivity. These results show the need to correctly assess spatial dispersion effects in the development of plasmonic devices at the low THz band.**

***Index Terms*—Graphene, plasmonics, spatial dispersion, surface waves.**

I. Introduction

THE propagation of electromagnetic waves along graphene sheets has recently attracted significant attention [1]–[3]. Graphene, thanks to its interesting electrical and optical properties [4], provides new possibilities for surface-wave propagation at optical, infrared, and low THz frequencies [3], [5]. Specifically, graphene enables the development of novel plasmonic devices at relatively low frequencies [3], [6]–[8] in contrast with noble metals which only allows plasmonic propagation in the visible range [9], [10]. In addition, graphene is inherently tunable, via the application of an electrostatic or magnetostatic bias field, leading to novel reconfiguration possibilities [5], [11]. Many research groups have theoretically studied the propagation of plasmons (i.e., electromagnetic waves propagating at the interface between a conductor and a dielectric) along graphene [1]–[3], [12], [13]. Also, different configurations have recently been proposed to improve the characteristics of this propagation, including parallel plate pairs [12], [14] or waveguides [15]. Furthermore, recent studies have demonstrated enhanced transmission through a stack of monolayer graphene sheets [16]. However, though graphene is known to be spatially dispersive [17], spatial dispersion has usually been neglected in works related to wave propagation at low THz frequencies. In [2], a nonlocal model of the graphene tensor conductivity, valid in the frequency range where intraband contributions of graphene dominate, was proposed. Based on this model, [2] also predicted that spatial dispersion would become significant for extremely slow surface waves. In case of graphene in free space, this occurs when interband contributions of graphene dominate (moderate to high THz frequencies). This model was also recently employed in [18] to study spatial dispersion effects in graphene-based parallel-plate waveguides, focusing on the particular case of graphene with uniform zero chemical potential.

In this paper, we investigate the propagation of surface waves along a spatially dispersive graphene sheet, including substrate effects, and we show that spatial dispersion affects the behavior of these waves even in the low THz range. The sheet is characterized using the graphene tensorial conductivity obtained by applying the nonlocal spatially dispersive model of graphene presented in [2], [19], and [20], valid in the absence of external magnetostatic bias field, at frequencies where intraband contributions of graphene dominate, and for any value of graphene chemical potential. This model has been derived from the semi-classical Boltzmann transport equation assuming a linear electron dispersion, and uses the relaxation-time (RTA, see [21]) and the so-called k_ρ-low approximations. Therefore, it is accurate in the case of relatively low values of the propagation constant k_ρ, while providing approximate results for moderate values of k_ρ. Here, we employ this model instead of the general spatially dispersive graphene conductivity model described in [17] because it enables obtaining closed-form expressions for the propagation constant of spatially dispersive surface waves propagating on graphene sheets, thereby providing physical insight into their properties. The operator components of the conductivity tensor are then mapped onto the admittances of a rigorous Green's function-based equivalent circuit of graphene [22]. These equivalent admittances, which are similar to those found in the analysis of frequency-selective surfaces [23], [24], analytically show that the influence of spatial dispersion directly depends on the square of the wave propagation constant (k_ρ). Then, a transverse resonance equation (TRE) [25] is imposed to compute the dispersion relation of surface waves along spatially dispersive graphene. Similar to the case of non-spatially dispersive graphene sheets, transverse-electric (TE)

Manuscript received September 08, 2012; manuscript revised January 07, 2013; accepted March 16, 2013. Date of publication March 22, 2013; date of current version July 01, 2013. This work was supported in part by the Swiss National Science Foundation (SNSF) under Grant 133583 and in part by the EU FP7 Marie-Curie IEF grant "Marconi," with ref. 300966.

J. S. Gomez-Diaz and J. Perruisseau-Carrier are with the Adaptive Micro-NanoWave Systems, LEMA/Nanolab, École Polytechnique Fédérale de Lausanne, Lausanne 1015, Switzerland. (e-mail: juan-sebastian.gomez@epfl.ch; julien.perruisseau-carrier@epfl.ch).

J. R. Mosig is with the Electromagnetics and Acoustics Laboratory (LEMA), École Polytechnique Fédérale de Lausanne, Lausanne 1015, Switzerland. (e-mail: juan.mosig@epfl.ch).

Color versions of one or more of the figures in this paper are available online at http://ieeexplore.ieee.org.

Digital Object Identifier 10.1109/TAP.2013.2254443

and transverse-magnetic (TM) modes are supported. Analytical dispersion relations are provided for TM and TE surface waves propagating along a graphene sheet embedded into a homogeneous medium, while approximate expressions are given for the case of graphene surrounded by two different dielectrics. The derived dispersion relations analytically show that the permittivity of the surrounding media, operation frequency, and spatial dispersion similarly contribute to determine the characteristics of k_ρ, suggesting that the influence of graphene spatial dispersion in the propagating waves may be strongly affected by the environment of the sheet. Numerical results confirm that spatial dispersion is an important mechanism for wave propagation along graphene sheets, leading to surface modes that can significantly differ from those found neglecting spatial dispersion. These features, which include variations in the mode confinement and higher losses, should be rigorously taken into account in the development of novel plasmonic devices at the low THz band.

This paper is organized as follows. Section II derives the analytical relations between the admittances of a Green's function-based equivalent circuit of graphene and the components of the spatially dispersive conductivity tensor. Then, Section III computes the dispersion relation of surface waves propagating along graphene, providing analytical expressions for the case of a graphene sheet embedded into an homogeneous media. Section IV discusses the characteristics of surface waves along spatially dispersive graphene, taking into account the surrounding media. Finally, conclusions and remarks are provided in Section V.

II. Equivalent Circuit ofa Spatially Dispersive Graphene Sheet

Let us consider an infinitesimally thin graphene sheet in the plane $z = 0$ and separating two media, as illustrated in Fig. 1(a). The sheet is characterized by the conductivity tensor $\overline{\overline{\sigma}}$, obtained by applying a spatially dispersive (non-local) model of graphene [2] in the absence of external magnetostatic biasing fields ($\vec{B}_0 = 0$). This anisotropic conductivity reads

$$\overline{\overline{\sigma}}(\omega, \mu_c, \tau, T) = \begin{pmatrix} \sigma_{x'x'} & \sigma_{x'y'} \\ \sigma_{y'x'} & \sigma_{y'y'} \end{pmatrix} \tag{1}$$

where T is the temperature, τ is the electron relaxation time, μ_c is the chemical potential, and ω is the angular frequency. Due to the spatial dispersion of graphene, the conductivity components become operators [2], [26]

$$\sigma_{x'x'} = \sigma_{lo} + \alpha_{sd}\frac{\partial^2}{\partial x'^2} + \beta_{sd}\frac{\partial^2}{\partial y'^2} \tag{2}$$

$$\sigma_{y'y'} = \sigma_{lo} + \beta_{sd}\frac{\partial^2}{\partial x'^2} + \alpha_{sd}\frac{\partial^2}{\partial y'^2} \tag{3}$$

$$\sigma_{x'y'} = \sigma_{y'x'} = 2\beta_{sd}\frac{\partial^2}{\partial x' \partial y'} \tag{4}$$

where

$$\sigma_{lo} = \frac{-jq_e^2 k_B T}{\pi\hbar^2(\omega - j\tau^{-1})} \ln\left[2\left(1 + \cosh\left(\frac{\mu_c}{k_B T}\right)\right)\right] \tag{5}$$

$$\alpha_{sd} = \frac{-3v_F^2\sigma_{lo}}{4(\omega - j\tau^{-1})^2}, \quad \beta_{sd} = \frac{\alpha_{sd}}{3}. \tag{6}$$

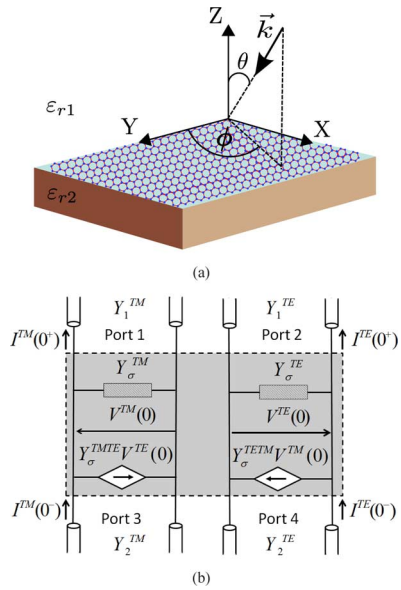

Fig. 1. (a) Spatially dispersive graphene sheet on a dielectric substrate under arbitrary plane-wave incidence and (b) its equivalent transmission-line model [22].

k_B is Boltzmann's constant, q_e is the electron charge, v_F is the Fermi velocity ($\approx 10^6$ m/s in graphene), and the subscripts "lo" and "sd" have been included to denote local and spatially dispersive (non-local) terms. Note the presence of a minus sign in α_{sd}, which was not included in [2] due to a typo [26]. It is worth mentioning that this model is insensitive to the orientation of the graphene lattice, and that anisotropy arises as a response of the material to the excitation, as usually occurs with spatial dispersion [2], [26]. Consequently, the coordinate system employed in the anisotropic conductivity [$x' - y'$, see (2)–(4)] is related to the excitation (i.e., $\sigma_{x'x'}$ and $\sigma_{y'y'}$ provide the response parallel to the $E_{x'}$ and $E_{y'}$ fields), with x' and y' being arbitrary perpendicular directions in the infinite sheet. Importantly, (2) and (6) are only strictly valid at frequencies where the intraband contributions of graphene conductivity dominate, usually the low THz regime. Intraband contributions correspond to electron transitions between different energy levels in the same band (valence or conduction), while interband contributions are related to electron transitions between different bands. The latter phenomenon becomes significant as frequency increases due to the higher photon energy [21].

A rigorous equivalent circuit of an anisotropic graphene sheet sandwiched between two media is shown in Fig. 1(b) [22]. This four-port circuit relates input and output TE and TM waves through equivalent shunt admittances (Y_σ^{TE} and Y_σ^{TM}, respectively), and the cross-coupling between the two polarizations through voltage-controlled current generators, with coefficients $Y_\sigma^{TE/TM}$ and $Y_\sigma^{TM/TE}$ for TE-TM and TM-TE coupling, respectively. The relation between the anisotropic conductivity of graphene and these admittances was provided in [22] for the case of a local model of graphene (i.e., when anisotropy is due to an external magnetostatic bias field). However, spatial dispersion effects have not been considered so far.

Here, we analytically obtain the admittances of the equivalent circuit shown in Fig. 1(b) using a nonlocal (spatially dispersive)

model of graphene. For this purpose, we include the operator components of the tensor conductivity, (2)–(4), into the transmission-line network formalism for computing dyadic Green's functions in stratified media [22], [27]. For the admittances derivation, we consider a uniform plane wave impinging on the graphene sheet from an arbitrary direction (θ, ϕ) of medium 1 [see Fig. 1(a)], and then we use the corresponding auxiliary coordinate system for the conductivity tensor. The incoming wave has a wave number $\vec{k} = k_x\hat{e}_x + k_y\hat{e}_y + k_z\hat{e}_z$, where $k_x = k_1\cos(\phi)\sin(\theta)$, $k_y = k_1\sin(\phi)\sin(\theta)$, $k_z = k_1\cos(\theta)$, $\hat{e}_x, \hat{e}_y, \hat{e}_z$ are unit vectors, and $k_0 = 2\pi/\lambda_0$ and $k_1 = \sqrt{\varepsilon_{r1}}k_0$ are the wavenumbers of free space and medium 1, respectively. Imposing boundary conditions in the graphene plane and following the approach described in [22] and [27], these admittances can be written as

$$Y_\sigma^{\mathrm{TE}}(k_\rho) = \sigma_{lo} + k_\rho^2[\alpha_{sd} + \beta_{sd}] \tag{7}$$

$$Y_\sigma^{\mathrm{TM}}(k_\rho) = \sigma_{lo} + k_\rho^2[\alpha_{sd} + \beta_{sd}] \tag{8}$$

$$Y_\sigma^{\mathrm{TE/TM}}(k_\rho) = Y_\sigma^{\mathrm{TM/TE}}(k_\rho) = 0 \tag{9}$$

where $k_\rho^2 = k_x^2 + k_y^2$ is the propagation constant of the wave traveling along the graphene sheet.

The importance of (7)–(9) is two fold. First, they analytically indicate that the influence of spatial dispersion is directly proportional to k_ρ^2. Consequently, this phenomenon will be more important for very slow waves $(k_\rho \gg k_0)$, which usually appear at moderately high THz frequencies (where interband contributions of graphene dominate and (2)–(4) are not strictly valid [2]). However, note that slow waves can also be obtained in graphene sheets at low THz frequencies by using substrates with a high permittivity constant [3]. Second, the equivalent admittances do not depend on the direction of propagation of the wave along the sheet (ϕ) and there is no coupling between the TM and TE modes. This is in agreement with the nonlocal model of graphene employed in this development [2], [26] which assumes an isotropic infinite surface where spatial dispersion arises in response to a given excitation.

III. Dispersion Relation for a Spatially Dispersive Graphene Sheet

The dispersion relation of surface waves on a spatially dispersive graphene sheet sandwiched between two different media can be obtained by imposing a transverse resonance equation [25] to the equivalent circuit shown in Fig. 1(b). The solution of the TRE provides the propagation constant k_ρ of the surface wave propagating along the sheet. Following the approach described in [13], the desired dispersion relation can be obtained as

$$\left(Y_1^{\mathrm{TE}} + Y_2^{\mathrm{TE}} + Y_\sigma^{\mathrm{TE}}\right)\left(Y_1^{\mathrm{TM}} + Y_2^{\mathrm{TM}} + Y_\sigma^{\mathrm{TM}}\right) = 0 \tag{10}$$

where

$$Y_1^{\mathrm{TE}} = \frac{k_{z_1}}{\omega\mu_0}, \quad Y_2^{\mathrm{TE}} = \frac{k_{z_2}}{\omega\mu_0}, \quad Y_1^{\mathrm{TM}} = \frac{\omega\varepsilon_{r_1}\varepsilon_0}{k_{z_1}}$$
$$Y_2^{\mathrm{TM}} = \frac{\omega\varepsilon_{r_2}\varepsilon_0}{k_{z_2}}, k_{z_1} = \pm\sqrt{k_1^2 - k_\rho^2}, k_{z_2} = \pm\sqrt{k_2^2 - k_\rho^2}$$
$$k_1 = \sqrt{\varepsilon_{r_1}}k_0, \quad \text{and} \quad k_2 = \sqrt{\varepsilon_{r_2}}k_0 \tag{11}$$

are the TE and TM admittances, transverse propagation constant, and wave number of media 1 and 2, respectively.

Equation (10) does not generally admit any analytical solution and must be solved using numerical methods [28]. Importantly, the mathematical solutions of this equation must be carefully checked to verify that they correspond to physical modes. Specifically, physical modes must fulfill the law of energy conservation (i.e., surface waves cannot be amplified while propagating along the structure), and the Sommerfeld boundary radiation condition [25]. Also, note that the solution of (10) leads to the propagation constant of a TE or a TM mode, as in the case of isotropic graphene [1]. These cases are examined below.

A. TM Modes

The dispersion relation for TM modes propagating along a spatially dispersive graphene sheet can be obtained by solving $Y_1^{TM} + Y_2^{TM} + Y_\sigma^{TM} = 0$ [see (10)]. This equation may be expressed as

$$\frac{\omega\varepsilon_{r1}\varepsilon_0}{\sqrt{\varepsilon_{r1}k_0^2 - k_\rho^2}} + \frac{\omega\varepsilon_{r2}\varepsilon_0}{\sqrt{\varepsilon_{r2}k_0^2 - k_\rho^2}} = -\left[\sigma_{lo} + k_\rho^2(\alpha_{sd} + \beta_{sd})\right]. \tag{12}$$

If the graphene sheet is embedded into a homogeneous host medium, i.e., $\varepsilon_{r1} = \varepsilon_{r2} = \varepsilon_r$, the dispersion relation can be simplified to

$$k_\rho^6 + k_\rho^4\left[\frac{2\sigma_{lo}}{\alpha_{sd} + \beta_{sd}} - \varepsilon_r k_0^2\right] - k_\rho^2\left[\frac{2\varepsilon_r\sigma_{lo}k_0^2(\alpha_{sd} + \beta_{sd}) - \sigma_{lo}^2}{(\alpha_{sd} + \beta_{sd})^2}\right] + \frac{4\omega^2\varepsilon_r^2\varepsilon_0^2 - \varepsilon_r k_0^2\sigma_{lo}^2}{(\alpha_{sd} + \beta_{sd})^2} = 0 \tag{13}$$

which has six complex roots but can be solved analytically using standard techniques [29]. Also, considering two different media and assuming the usual nonretarded regime $(k_\rho \gg k_0)$, (12) reduces to

$$k_\rho^3 + k_\rho\frac{\sigma_{lo}}{\alpha_{sd} + \beta_{sd}} - j\omega\frac{\varepsilon_0(\varepsilon_{r1} + \varepsilon_{r2})}{\alpha_{sd} + \beta_{sd}} = 0 \tag{14}$$

which is a cubic equation with three complex roots. Note that the operation frequency (ω) and the permittivity of the surrounding media (ε_{r1} and ε_{r2}) only appear in the free term of (14), where they multiply each other. Therefore, the behavior of surface waves propagating along a graphene sheet is mainly determined by this product, suggesting that similar responses will be obtained for larger frequencies if the permittivity is simultaneously reduced, or vice-versa. Similar conclusions are reached by closely examining (13). However, this does not mean that frequency and permittivity are fully interchangeable since graphene conductivity itself is frequency dependent. In the asymptotic limit $\omega\varepsilon_0(\varepsilon_{r1} + \varepsilon_{r2}) \gg k_\rho\sigma_{lo}$, (14) can be solved analytically and yields

$$k_\rho \approx \sqrt[3]{j\omega\varepsilon_0\frac{(\varepsilon_{r1} + \varepsilon_{r2})}{\alpha_{sd} + \beta_{sd}}}. \tag{15}$$

This equation shows that in the limit of very high frequencies, or a large permittivity of the surrounding media, spatial dispersion will be the main phenomenon governing wave propagation. However, note that interband contributions of graphene conductivity, which are dominant at such high frequencies, have not been considered in this analysis.

In the absence of spatial dispersion ($\alpha_{sd} = \beta_{sd} = 0$), (14) simplifies to the usual expression [3]

$$k_\rho \approx j\omega\varepsilon_0 \frac{(\varepsilon_{r1} + \varepsilon_{r2})}{\sigma_{lo}}. \tag{16}$$

The cutoff frequency of the propagating TM modes can be obtained by numerically finding the lowest frequencies which fulfill (12). A very good approximation is obtained by identifying the frequency range of $Im(\sigma_{lo}) < 0$, which is the condition for TM mode propagation along a nonspatially dispersive graphene sheet [1]. Note that the cutoff frequency of the supported TM modes mainly depends on the characteristics of the local conductivity of graphene, which can be externally controlled by tuning the chemical potential of graphene via the field effect. See (17) at the bottom of the page.

B. TE Modes

The dispersion relation for TE modes propagating along a spatially dispersive graphene sheet can be expressed as

$$\frac{\sqrt{\varepsilon_{r1}k_0^2 - k_\rho^2}}{\omega\mu_0} + \frac{\sqrt{\varepsilon_{r2}k_0^2 - k_\rho^2}}{\omega\mu_0} = -\left[\sigma_{lo} + k_\rho^2(\alpha_{sd} + \beta_{sd})\right]. \tag{18}$$

In case the graphene sheet is embedded into a homogeneous medium, with $\varepsilon_{r1} = \varepsilon_{r2} = \varepsilon_r$, this equation admits the analytical solution shown in (17).

Similarly, as in the case of TM modes, the cutoff frequency of TE modes mainly depends on the local conductivity of graphene σ_{lo}. Specifically, an accurate condition for the propagation of these modes along a graphene sheet is $Im(\sigma_{lo}) > 0$ [1].

IV. Numerical Results

In this section, we investigate the influence of spatial dispersion in the characteristics of surface waves propagating along a graphene sheet, taking into account the surrounding media. Specifically, we study the normalized propagation constant (mode confinement $Re(k_\rho/k_0)$ and losses $Im(k_\rho/k_0)$) of TM waves along spatially dispersive graphene, and compare the results with the ones obtained by neglecting spatial dispersion [1]. In the numerical study, we focus our results on TM waves, which are known to be of interest for plasmonic devices [3], [6]. Though TE surface waves are also supported by graphene sheets, they present similar characteristics to waves propagating in free space (i.e., $k_\rho \approx k_0$) [1] and, thus, have less practical interest. We compute reference results for a nonspatially dispersive graphene sheet considering intraband and $\mathrm{intraband} + \mathrm{interband}$ contributions of conductivity. The aim of this comparison is to identify which phenomenon (spatial dispersion or interband contributions) becomes dominant as frequency increases. Furthermore, we will also investigate the influence of spatial dispersion in the propagating surface waves as a function of different parameters of graphene. Our numerical simulations consider graphene at $T = 300\,^\circ$ K and a relaxation time of 0.135 ps, in agreement with measured values [3], [4]. The results shown here have been obtained numerically [solving (12)] or analytically [from (13)], depending on the surrounding media of graphene. Besides, note that the analytical solution of (14) leads to results with differences smaller than 0.1% with respect to those numerically obtained from (12), further confirming the validity of this expression.

First, we consider the case of a graphene sheet with chemical potential $\mu_c = 0.05$ eV surrounded by air. Fig. 2(a) and (b) shows the normalized propagation constant and losses of surface waves propagating along the spatially dispersive sheet. Specifically, two modes are supported by the structure, which are the physical solutions of (13). The first mode (denoted as "SD—mode 1") presents extremely similar characteristics compared to a TM surface mode supported by a nonspatially dispersive graphene sheet, computed considering only intraband contributions of graphene. Fig. 2(a) and (b) also include similar computations but considering interband contributions as well. The effect of interband contribution becomes visible at high frequencies, increasing the losses of the mode. Thus, we can conclude that for this particular case, the influence of spatial dispersion is negligible in the low THz range. In [2], similar conclusions were obtained by analyzing, in the transformed Fourier domain, the ratio between graphene conductivity and the terms related to spatial dispersion. Interestingly, here we also observe that a second mode, denoted as "SD—mode 2," is supported due to the presence of spatial dispersion. It is observed that this mode is extremely lossy in the band of interest, which greatly limits its possible use in practical applications.

Fig. 2(c) and (d) presents a similar study, but now consider a graphene sheet that has been embedded into homogeneous material with $\varepsilon_r = 11.9$. The results demonstrate that spatial dispersion becomes the dominant mechanism of wave propagation in this case, even at relatively low frequencies, drastically changing the behavior of the two modes supported by the graphene sheet. At low frequencies, the first mode ("SD—mode 1") presents very similar characteristics compared to a TM surface mode along a graphene sheet, neglecting spatial dispersion. However, the confinement and losses of the mode increase with frequency. At around 2 THz, losses

$$k_\rho = \pm\sqrt{\frac{-\sigma_{lo}\omega^2\mu_0^2(\alpha_{sd} + \beta_{sd}) + 2(1 \pm \sqrt{1 + \omega^2\mu_0^2(\alpha_{sd} + \beta_{sd})[\sigma_d + (\alpha_{sd} + \beta_{sd})\varepsilon_r k_0^2]}}{\omega^2\mu_0^2(\alpha_{sd} + \beta_{sd})^2}}. \tag{17}$$

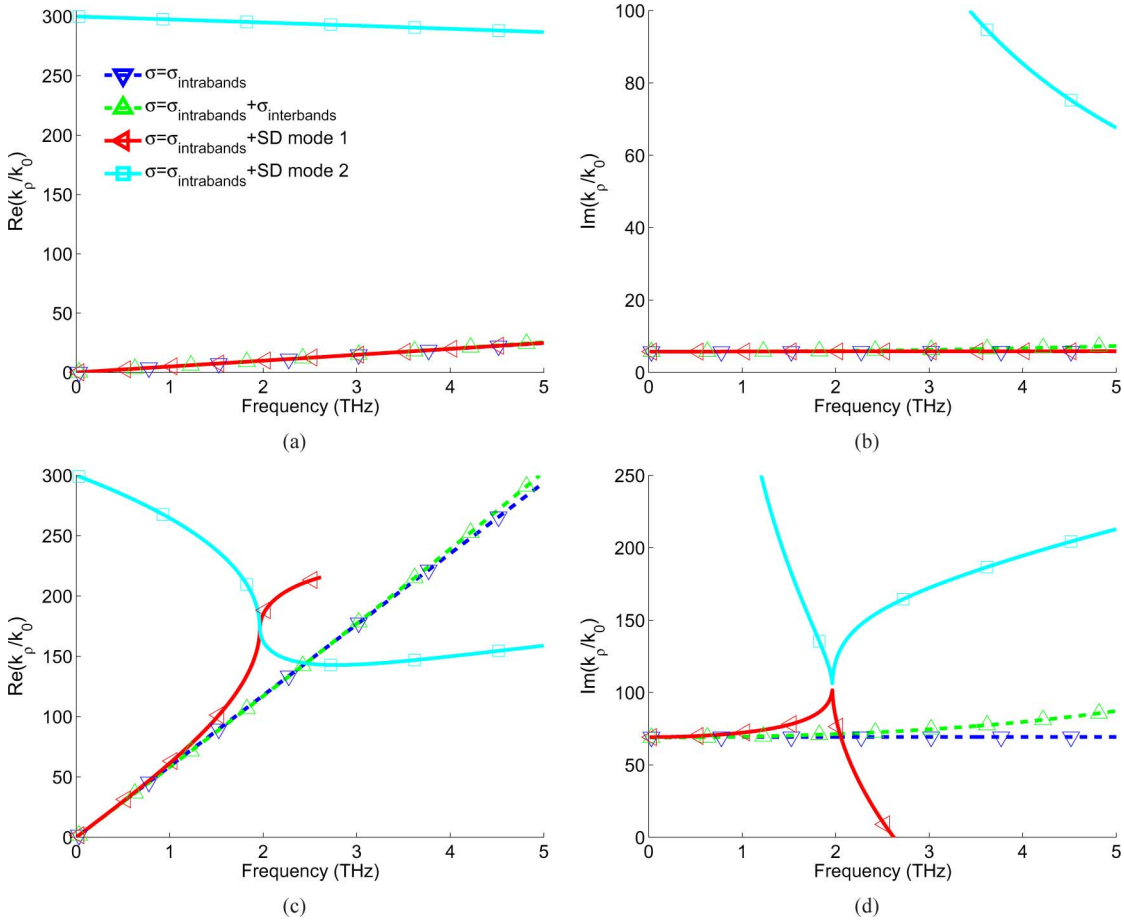

Fig. 2. Characteristics of surface waves propagating along a spatially dispersive (SD) graphene sheet versus frequency computed by using (13). Reference results, related to the surface waves propagating along nonspatially dispersive graphene [1] have been computed by taking into account intraband and $\mathrm{intraband} + \mathrm{interband}$ contributions of conductivity, which are included for comparison purposes. (a) and (b) show the normalized propagation constant and losses of surface waves along a free-space standing graphene sheet. (c) and (d) show the normalized propagation constant and losses of surface waves along a graphene sheet embedded into homogeneous media with $\varepsilon_r = 11.9$. Graphene parameters are $\mu_c = 0.05$ eV, $\tau = 0.135$ ps, and $T = 300\,^\circ$ K.

exponentially decrease, thus leading to a nonphysical improper mode at frequencies above 2.5 THz. The behavior of the second mode ("SD—mode 2") is also affected by spatial dispersion. As frequency increases, the confinement and losses of the mode decrease. Above 2 THz, the confinement of the mode remains relatively constant and losses slightly increase. It should be noted that although the phase constant of modes 1 and 2 intersects at around 2 THz, their attenuation constants are different at that frequency, thus allowing them to clearly identify the modes. Besides, note that the frequency where the phase constant of the modes intersects defines the frequency region where the influence of spatial dispersion starts to be dominant. Furthermore, mode coupling occurs between the two modes supported by the graphene sheet. This coupling is governed by the occurrence of a complex-frequency-plane branch point that migrates across the real frequency axis [30], [31].

Importantly, the influence of spatial dispersion on the characteristics of the supported modes strongly depends on the features of graphene. As an illustration, Fig. 3 presents the phase constant of the two modes propagating along a graphene sheet [with the parameters employed in Fig. 2(c)] as a function of the chemical potential μ_c and the relaxation time τ. We observe in Fig. 3(a) that the chemical potential controls the frequency where the phase constant of the two modes intersects, which is the frequency where spatial dispersion starts to have a dominant effect on the behavior of the modes. Note that an increase of μ_c upshifts this frequency. In addition, Fig. 3(b) shows that the relaxation time of graphene determines the phase constant of the surface waves in the frequency region where spatial dispersion is dominant. Increasing τ modifies the phase constant of the modes, which tend to have a similar behavior versus frequency, and reduces their attenuation losses.

For the sake of completeness, we present the study of surface waves propagating along spatially dispersive graphene in Fig. 4(a), but considering now a constant frequency and varying the permittivity of the surrounding media. It is worth mentioning that, in practice, the material permittivity might affect graphene relaxation time [21], but this effect is neglected here for convenience. Fig. 4(a) and (b) presents the normalized phase and attenuation constants of surface waves propagating along graphene for a fixed frequency of 1 THz. The first mode is extremely similar to a TM surface mode along graphene, neglecting spatial dispersion. As expected from (14), mode confinement and losses increases when the dielectric constant is very high. It is interesting that there are many similarities in the behavior of the different modes in this situation and in the

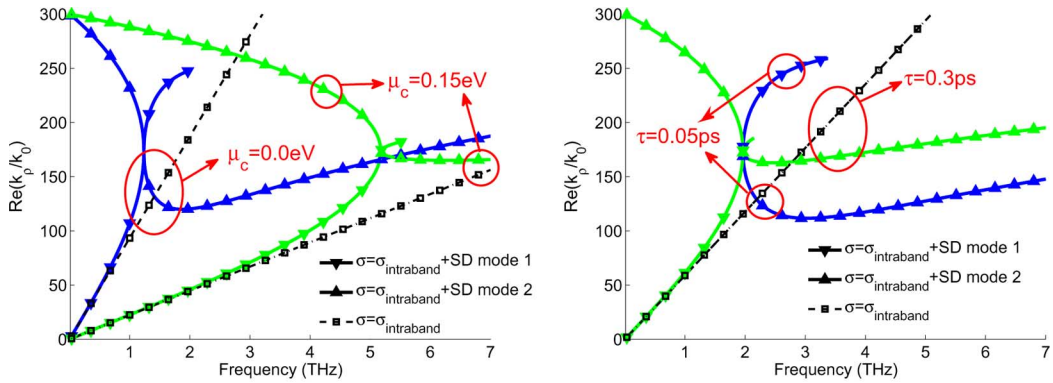

Fig. 3. Normalized phase constant of surface waves propagating on a spatially dispersive graphene sheet versus frequency, computed for different values of (a) chemical potential (using $\tau = 0.135$ ps) and (b) relaxation time (using $\mu_c = 0.05$ eV). Reference results, related to surface waves on a nonspatially dispersive graphene sheet, were computed by only taking into account intraband contributions of conductivity [1], which are included for comparison purposes. The permittivity of the surrounding media is $\varepsilon_r = 11.9$ and temperature is $T = 300\,^\circ$ K.

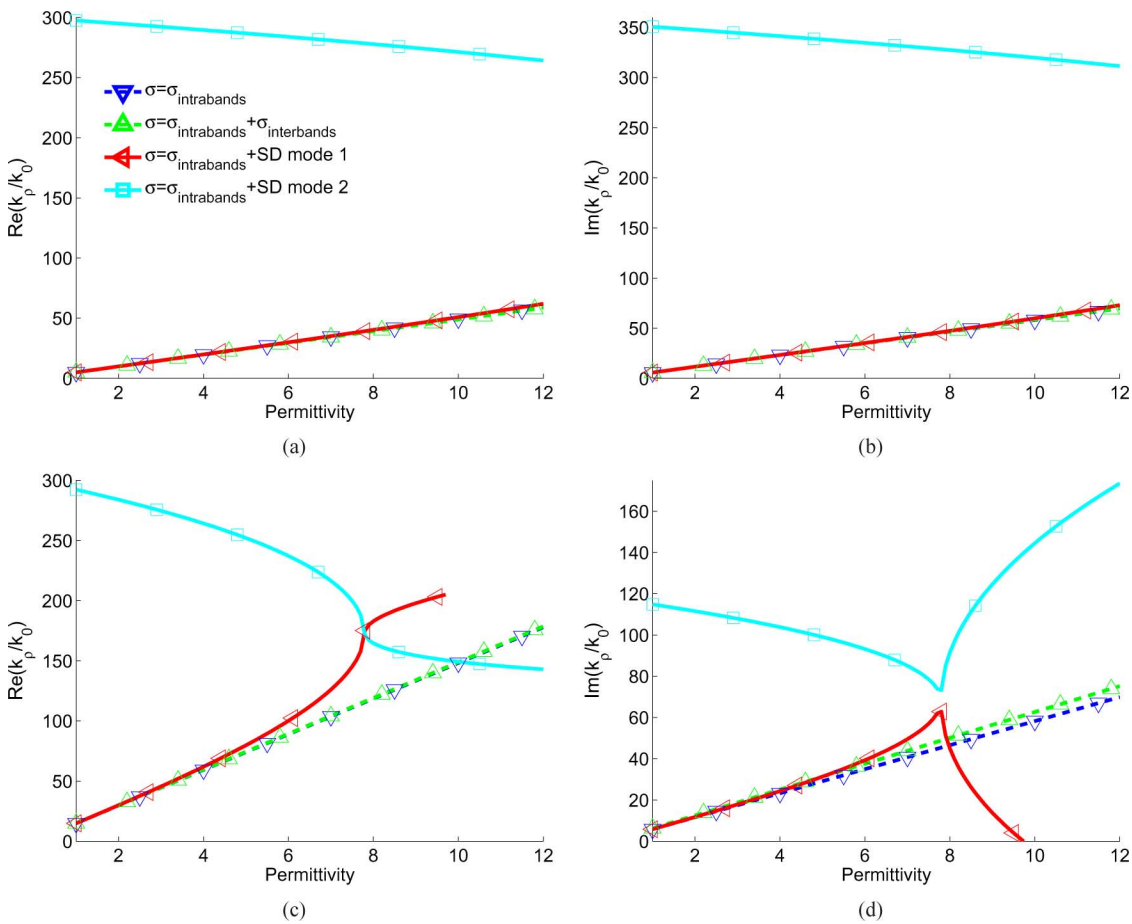

Fig. 4. Characteristics of surface waves propagating along a spatially dispersive (SD) graphene sheet as a function of surrounding media permittivity, computed using (13). Reference results, related to surface waves propagating along nonspatially dispersive graphene [1] are computed by taking into account intraband and $\mathrm{intraband} + \mathrm{interband}$ contributions of conductivity, which are included for comparison purposes. (a) and (b) show the normalized propagation constant and losses of the surface waves at 1 THz. (c) and (d) show the normalized propagation constant and losses of the surface waves at 3 THz. Graphene parameters are $\mu_c = 0.05$ eV, $\tau = 0.135$ ps, and $T = 300\,^\circ$ K.

previous example, where the surrounding media was constant (with a low permittivity value of $\varepsilon_r = 1$) and frequency was increased. Moreover, in Fig. 4(c) and (d), we present the same study but at the higher frequency of 3 THz. It is observed that spatial dispersion becomes the dominant phenomenon for wave propagation. In fact, it leads to propagating modes with similar behavior as in the previous example [see Fig. 2(c) and (d)], where we used a fixed large value of permittivity ($\varepsilon_r = 11.9$) and varied frequency. This example confirms that by neglecting the frequency dependence of graphene conductivity, permittivity and frequency play a similar role in the characteristics of surface waves propagating along spatially dispersive graphene.

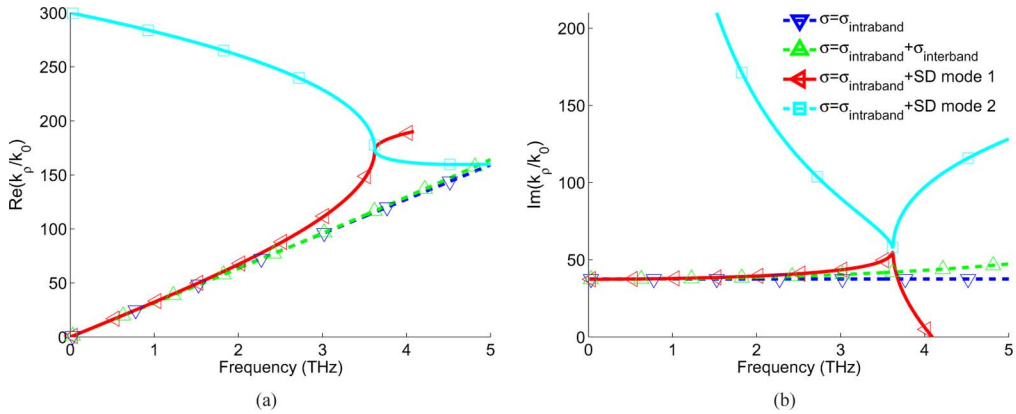

Fig. 5. Characteristics of surface waves propagating along a spatially dispersive (SD) graphene sheet deposited on a silicon substrate ($\varepsilon_r = 11.9$) versus frequency, computed by using (12). Reference results, related to surface waves propagating along nonspatially dispersive graphene [1], are computed by taking into account intraband and $\mathrm{intraband} + \mathrm{interband}$ contributions of conductivity, and are included for comparison purposes. (a) and (b) show the normalized propagation constant and losses of the surface waves, respectively. Graphene parameters are similar to those of Fig. 2.

Finally, we investigate in Fig. 5 the propagation of surface waves in a more realistic scenario, which consists of a spatially dispersive graphene sheet deposited on a silicon substrate ($\varepsilon_r = 11.9$), as illustrated in Fig. 1(a). Very similar behavior compared to the previous examples is obtained. Furthermore, these results demonstrate that the variation of the surrounding media directly controls the frequency range where spatial dispersion is noticeable. Analyzing these variations, we can conclude that increasing the permittivity of the media surrounding graphene downshifts the frequencies where the spatial dispersion phenomenon dominates wave propagation.

V. Conclusion

The propagation of surface waves along a spatially dispersive graphene sheet has been addressed. The analysis, that was based on the transverse resonance method extended to handle graphene spatial dispersion, was enabled to obtain the desired dispersion relation for surface waves propagating along a graphene sheet. Our results have demonstrated that spatial dispersion is an important mechanism which contributes to the propagation of surface waves along graphene sheets and that its influence cannot be systematically neglected. In fact, the presence of spatial dispersion at frequencies where intraband contributions of graphene dominate lead to surface waves with very different characteristics from those propagating along graphene sheets neglecting spatial dispersion. In addition, the frequency region where spatial dispersion is noticeable depends on the surrounding media and the chemical potential of graphene, while the features of the propagating surfaces waves are mainly determined by the relaxation time. These results demonstrate that the influence of spatial dispersion on surface waves propagating on graphene sheets should be rigorously taken into account for the development of novel plasmonic devices in the low THz range.

The study presented here has been based on a theoretical model of graphene which characterizes it as an infinitesimally thin layer with an associated tensor conductivity. This model uses the relaxation time approximation, only takes into account intraband contributions of graphene, and is valid in the absence of external magnetostatic biasing fields. Further work is needed in this area to analyze the behavior of surface waves along spatially dispersive graphene when these assumptions are not satisfied.

Acknowledgment

The authors would like to thank Prof. G. W. Hanson (University of Wisconsin-Milwaukee, USA), Dr. Garcia-Vigueras, and Dr. E. Sorolla-Rosario (École Polytechnique Fédérale de Lausanne, Switzerland) for their fruitful discussions.

References

[1] G. W. Hanson, "Dyadic green's functions and guided surface waves for a surface conductivity of graphene," *J. Appl. Phys.*, vol. 103, pp. 064302–064302, 2008.
[2] G. W. Hanson, "Dyadic green's functions for an anisotropic non-local model of biased graphene," *IEEE Trans. Antennas Propag.*, vol. 56, no. 3, pp. 747–757, Mar. 2009.
[3] M. Jablan, H. Buljan, and M. Soljacic, "Plasmonics in graphene at infrared frequencies," *Phys. Rev. B*, vol. 80, pp. 245435–245435, 2009.
[4] K. S. Novoselov, A. K. Geim, S. V. Morozov, D. Jiang, Y. Zhang, S. V. Dubonos, I. V. Grigorieva, and A. A. Firsov, "Electric field effect in atomically thin carbo filts," *Science*, vol. 306, pp. 666–669, 2004.
[5] A. Vakil and N. Engheta, "Transformation optics using graphene," *Science*, vol. 332, pp. 1291–1294, 2011.
[6] W. L. Barnes, A. Dereux, and T. W. Ebbesen, "Surface plasmon subwavelength optics," *Nature*, vol. 424, pp. 824–830, 2003.
[7] Y. V. Bludov, M. I. Vasilevskiy, and N. M. R. Peres, "Mechanism for graphene-based optoelectronic switches by tuning surface plasmon-polaritons in monolayer graphene," *Europhys. Lett.*, vol. 92, pp. 68001–68001, 2010.
[8] M. Tamagnone, J. S. Gomez-Diaz, J. R. Mosig, and J. Perruisseau-Carrier, "Reconfigurable thz plasmonic antenna concept using a graphene stack," *Appl. Phys. Lett.*, vol. 101, pp. 214102–214102, 2012.
[9] J. M. Pitarke, V. M. Silkin, E. V. Chulkov, and P. M. Echenique, "Theory of surface plasmons and surface-plasmon polaritons," *Rep. Prog. Phys.*, vol. 70, 2007.
[10] Y. Wang, E. W. Plummer, and K. Kempa, "Foundations of plasmonics," *Advances in Physics*, vol. 60, pp. 799–898, 2011.
[11] V. P. Gusynin, S. G. Sharapov, and J. P. Carbotte, "Magneto-optical conductivity in graphene," *J. Phys.: Condensed Matter*, vol. 19, no. 2, pp. 026222–026222, 2007.
[12] E. H. Hwang and J. D. Sarma, "Dielectric function, screening, and plasmons in two-dimensional graphene," *Phys. Rev. B*, vol. 75, pp. 205418–205418, May 2007.
[13] J. S. Gomez-Diaz and J. Perruisseau-Carrier, "Propagation of hybrid TM-TE plasmons on magnetically-biased graphene sheets," *J. Appl. Phys.*, vol. 112, pp. 124906–124906, 2012.
[14] G. W. Hanson, "Quasi-transverse electromagnetic modes supported by a graphene parallel-plate waveguide," *J. Appl. Phys.*, vol. 104, pp. 084314–084314, 2008.

[15] J. Christensen, A. Manjavacas, S. Thongrattanasiri, F. H. L. Koppens, and F. J. G. de Abajo, "Graphene plasmon waveguiding and hybridization in individual and paired nanoribbons," *ACS Nano.*, vol. 6, pp. 431–440, 2011.
[16] C. S. R. Kaipa, A. B. Yakovlev, G. W. Hanson, Y. R. Padooru, F. Medina, and F. Mesa, "Enhanced transmission with a graphene-dielectric microstructure at low-terahertz frequencies," *Phys. Rev. B*, vol. 85, pp. 245407–245407, 2012.
[17] L. A. Falkovsky and A. A. Varlamov, "Space-time dispersion of graphene conductivity," *Eur. Phys. J. B*, vol. 56, pp. 281–284, 2007.
[18] G. Lovat, P. Burghignoli, and R. Araneo, "Low-frequency dominant-mode propagation in spatially dispersive graphene nanowaveguides," *IEEE Trans. Electromagn. Compat.*, vol. 55, no. 2, pp. 328–333, Apr. 2013.
[19] G. Lovat, G. W. Hanson, R. Araneo, and P. Burghignoli, "Comparison of spatially dispersive models for dyadic interband conductivity of graphene," presented at the Eur. Conf. Antennas Propag., Gothenburg, Sweden, Apr. 2013.
[20] G. Lovat, G. W. Hanson, R. Araneoz, and P. Burghignoli*, Spatially Dispersive Intraband Conductivity Tensor and Quantum Capacitance of Graphene*, 2013.
[21] M. Dressel and G. Gruner*, Electrodynam. Solids*. Cambridge, U.K.: Cambridge Univ. Press, 2002.
[22] G. Lovat, "Equivalent circuit for electromagnetic interaction and transmission through graphene sheets," *IEEE Trans. Electromagn. Compat.*, vol. 54, no. 1, pp. 101–109, Feb. 2012.
[23] B. A. Munk*, Frequency Selective Surfaces: Theory and Design*. New York: Wiley, 2000.
[24] S. Maci, M. Caiazzo, A. Cucini, and M. Casaletti, "A pole-zero matching method for ebg surfaces composed of a dipole FSS printed on a grounded dielectric slab," *IEEE Trans. Antennas Propag.*, vol. 53, no. 1, pp. 70–81, Jan. 2005.
[25] R. E. Collin and F. J. Zucker*, Antenna Theory*. New York: McGraw-Hill, 1969.
[26] G. W. Hanson, Private communication, 2012.
[27] K. A. Michalski and J. R. Mosig, "Multilayered media Green's functions in integral equation formulations," *IEEE Trans. Antennas Propag.*, vol. 45, no. 3, pp. 508–519, Mar. 1997.
[28] W. H. Press, S. A. Teukolsky, W. T. Vetterling, and B. P. Flannery*, Numerical Recipes in Fortran 90, The Art of Parallel Scientific Computing*. Cambridge, U.K.: Cambridge University Press, 1996.
[29] L. A. Pipes and L. R. Harvill*, Applied Mathematics for Engineers and Physicist*, 3rd ed. New York: McGraw-Hill, 1971.
[30] G. W. Hanson and A. B. Yakovlev, "Investigation of mode interaction on planar dielectric waveguides with loss and gain," *Radio Sci.*, vol. 34, pp. 1349–1359, 1999.
[31] A. B. Yakovlev and G. W. Hanson, "Mode-transformation and mode-continuation regimes on waveguiding structures," *IEEE Trans. Microw. Theory Tech.*, vol. 48, no. 1, pp. 67–75, Jan. 2000.

Juan Sebastian Gomez-Diaz (S'07–M'12) was born in Ontur (Albacete), Spain, in 1983. He received the Ph.D. degree in electrical engineering from the Technical University of Cartagena (UPCT), Cartagena, Spain, in 2011.

In 2007, he joined the Telecommunication and Electromagnetic Group (GEAT), UPCT, as a Research Assistant on numerical methods based on the integral equation (IE) technique and their application to the analysis and design of microwave circuits and antennas. From 2007 to 2008, he was a visiting Ph.D. student at Poly-Grames, École Polytechnique de Montréal, Montréal, QC, Canada, where he was involved in the impulse-regime analysis of linear and nonlinear metamaterial-based devices and antennas. From 2009 to 2010, he was a visiting Ph.D. student at the Fraunhofer Institute for High Frequency Physics and Radar Techniques (FHR), Bonn, Germany, working on the modal analysis of leaky-wave antennas. In 2011, he joined EPFL as a Postdoctoral Fellow within the Adaptive MicroNanoWave System Group, where he currently develops his research activities.

Mr. Gomez-Diaz was the recipient of a FP7 IEF Marie-Curie Fellowship in 2012, the Colegio Oficial de Ingenieros de Telecomunicacin (COIT/AEIT) award for the best Spanish Ph.D. thesis in basic information and communication technologies in 2011, and the best Ph.D. thesis award from the Technical University of Cartagena in 2011. He serves as a reviewer for various journals on antennas and microwaves.

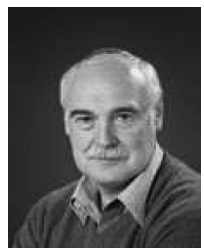

Juan R. Mosig (S'76–M'87–SM'94–F'99) was born in Cadiz, Spain. He received the Ph.D. degree in electrical engineering from Ecole Polytechnique Fdrale de Lausanne (EPFL), Lausanne, Switzerland, in 1983.

Since 1991, he has been a Professor at EPFL and since 2000, he has been the Head of the EPFL Laboratory of Electromagnetics and Acoustics (LEMA). In 1984, he was a Visiting Research Associate at the Rochester Institute of Technology, Rochester, NY. He has also held scientific appointments at the University of Rennes, Rennes, France; University of Nice, Nice, France; Technical University of Denmark; and University of Colorado at Boulder, CO, USA.

Dr. Mosig has been the Swiss Delegate for the European COST Antenna Actions since the 1980s and the Chair for the two last COST Antenna Actions 284 and IC0603 ASSIST (2003–2011). He is also a founding member and General Chair of the European Association on Antennas and Propagation (EurAAP), owner of the EuCAP Conference series. He is the originator of a successful annual workshop INTELECT on Computational Electromagnetics. He has authored four chapters in books on microstrip antennas and circuits and more than 120 reviewed papers. His research interests include electromagnetic theory, numerical methods, and planar antennas.

Julien Perruisseau-Carrier (S'07–M'09–SM'13) was born in Lausanne, Switzerland, in 1979. He received the M.Sc. and Ph.D. degrees in electrical engineering from the Ecole Polytechnique Fédérale de Lausanne (EPFL), Lausanne, Switzerland, in 2003 and 2007, respectively.

In 2003, he was with the University of Birmingham, Birmingham, U.K., first as a Visiting Student and then as a Short-Term Researcher. From 2004 to 2007, he was with the Laboratory of Electromagnetics and Acoustics (LEMA), EPFL, where he completed his Ph.D. while working on various EU-funded projects. From 2007 to 2011, he was an Associate Researcher with the Centre Tecnolgic de Telecomunicacions de Catalunya (CTTC), Barcelona, Spain. Since 2011, he has been a Professor at EPFL funded by the Swiss National Science Foundation, where he leads the group for Adaptive MicroNano Wave Systems. He has led various projects and workpackages at the National, European Space Agency, European Union, and industrial levels. Currently, he is Associate Editor of the IEEE TRANSACTIONS ON ANTENNAS AND PROPAGATION. He has authored more than 80 conference papers and over 40 journal papers. His main research interest concerns interdisciplinary topics related to electromagnetic waves from microwave to terahertz: dynamic reconfiguration, application of micro/nanotechnology, joint antenna-coding techniques, and metamaterials.

Mr. Perruisseau-Carrier was the recipient of the Raj Mittra Travel Grant 2010 presented by the IEEE Antennas and Propagation Society, and of the Young Scientist Award of the URSI International Symposium on Electromagnetic Theory, in 2007 and in 2013, respectively. He is the Swiss representative to URSI's commission "B Fields and waves."